Robust online motion planning via contraction theory and convex optimization

Robust Online Motion Planning via Contraction Theory and Convex Optimization

Sumeet Singh[1] Anirudha Majumdar[1] Jean-Jacques Slotine[2] Marco Pavone[1]

***Abstract*— We present a framework for online generation of robust motion plans for robotic systems with nonlinear dynamics subject to bounded disturbances, control constraints, and online state constraints such as obstacles. In an offline phase, one computes the structure of a feedback controller that can be efficiently implemented online to track *any* feasible nominal trajectory. The offline phase leverages *contraction theory* and *convex optimization* to characterize a fixed-size "tube" that the state is guaranteed to remain within while tracking a nominal trajectory (representing the center of the tube). In the online phase, when the robot is faced with obstacles, a motion planner uses such a tube as a robustness margin for collision checking, yielding nominal trajectories that can be safely executed, i.e., tracked without collisions under disturbances. In contrast to recent work on robust online planning using funnel libraries, our approach is not restricted to a fixed library of maneuvers computed offline and is thus particularly well-suited to applications such as UAV flight in densely cluttered environments where complex maneuvers may be required to reach a goal. We demonstrate our approach through simulations of a 6-state planar quadrotor navigating cluttered environments in the presence of a cross-wind. We also discuss applications of our approach to Tube Model Predictive Control (TMPC) and compare the merits of our method with state-of-the-art nonlinear TMPC techniques.**

I. Introduction

Despite significant progress in the field of motion planning, the problem of safe realtime planning for robots with nonlinear and underactuated dynamics subject to uncertainty has remained an outstanding challenge. A key difficulty is that uncertainty and disturbances in the dynamics force us to reason about the "funnel" of possible outcomes (see Fig. 1) that the disturbances may drive the system to, rather than a single planned trajectory.

The metaphor of a "funnel" was introduced to the robotics community in [1] and has inspired recent algorithms for *feedback motion planning* such as the LQR-Trees algorithm [2] which constructs a tree of locally stabilizing feedback controllers. However, LQR-Trees cannot handle scenarios in which the task and environment are unknown until runtime. Recently, the *funnel library* approach [3], [4] has been proposed to handle online geometric constraints (e.g., obstacles) that force the robot to replan in realtime. The approach leverages computational tools from convex optimization (namely sum-of-squares (SOS) programming) to compute, offline, a library of funnels around a set of nominal trajectories in which the state is *guaranteed* to remain despite bounded disturbances. These funnels are then sequentially composed online to avoid obstacles. However, this approach is restricted to employing a *fixed set* of trajectories computed offline. While the richness of the funnel library may be increased by exploiting invariances in the dynamics [4] or pre-computing a family of funnels parameterized by shifts to a nominal trajectory [5], one would ideally like to generate a funnel around *any* nominal trajectory generated online.

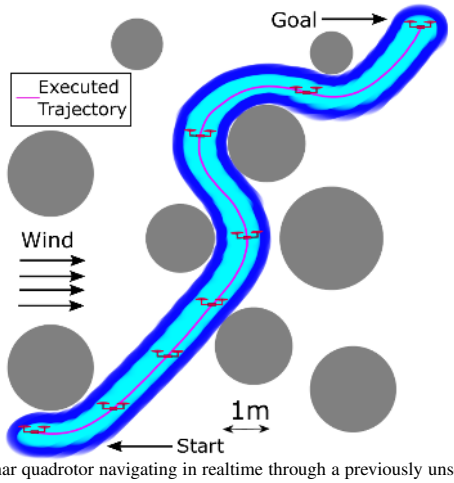

Fig. 1: A planar quadrotor navigating in realtime through a previously unseen cluttered environment in the presence of a cross-wind disturbance from the left. A nominal (disturbance-free) trajectory is generated online in response to obstacles reported in the environment such that the invariant tube (computed offline) recentered around the trajectory does not intersect obstacles. The actual executed trajectory veers to the right of the tube due to the cross-wind but remains within it as guaranteed by our analysis. The lighter shade represents the actual invariant tube while the darker shade is the tube inflated by the quadrotor arm length and is used for collision checking.

The goal of this paper is to propose an approach for doing precisely this. In particular, in an *offline* stage one synthesizes the structure of a tracking controller which can be efficiently implemented online to guarantee exponential convergence to *any* feasible nominal trajectory in the absence of disturbances. Additionally, the offline computation yields a fixed-size invariant "tube" (akin to a funnel) that can be recentered around any nominal trajectory as a guaranteed collision-free envelope in the presence of bounded disturbances. In the *online* phase, when the robot is faced with obstacles, one can use such a tube as a robustness margin during collision checking, thus leading to nominal trajectories that can be safely executed. We stress that this paper does not propose a new motion planning algorithm. Instead, it proposes a framework for using a standard motion planner as a "black

[1]Department of Aeronautics and Astronautics, Stanford University, Stanford, CA, 94305. {ssingh19, anirudha, pavone}@stanford.edu.

[2]Department of Mechanical Engineering, Massachusetts Institute of Technology, Cambridge, MA, 02139. {jjs@mit.edu}

This work was supported in part by NASA under the Space Technology Research Grants Program, Grant NNX12AQ43G, and by ONR under the Science of Autonomy Program, Contract N00014-15-1-2673. Sumeet Singh was supported by the Stanford Graduate Fellowship (SGF).

box" or "primitive routine" to enable the online generation of safe nominal motion plans that can be robustly executed.

Our approach has several advantages over prior work on robust motion planning. By explicitly enforcing safety in the online planning process, our approach is particularly suited to planning in previously unseen and tightly-constrained environments, where it might be difficult to find feasible solutions by sequencing a pre-computed set of maneuvers (Fig. 1). In contrast to the class of techniques that employ *linear* reachability analysis to conservatively approximate funnels/tubes for nonlinear systems by treating nonlinearities as bounded disturbances (see, e.g., [6]), our analysis directly reasons about intrinsic nonlinearities in the dynamics and thus has the potential to be less conservative for highly nonlinear systems. Further, our convex optimization-based approach carries a smaller computational burden than differential game formulations for computing reachable tubes [7], which require numerical solutions to PDEs. Finally, unlike [7], we do not assume that obstacles in the environment are known a priori but instead generate robust plans *online*.

The key idea behind our approach is to leverage *contraction theory* [8], a method for analyzing nonlinear systems by studying convergence between *pairs of trajectories*. This makes it particularly well-suited to the problem we consider here since it does not require us to commit to a particular nominal trajectory in order to analyze the stability properties of a feedback controller designed to track it. In particular, we design tracking controllers by using *control contraction metrics* (CCMs) [9], a generalization of control Lyapunov functions that can be computed using convex optimization.

Our formulation is closely related to Tube Model Predictive Control (TMPC), whereby one computes a tracking feedback controller (in our case, via CCMs) that keeps the state within an invariant "tube" (in our case, computed via contraction theory) around the nominal MPC trajectory despite disturbances. Indeed, we leverage the rich set of theoretical results from the TMPC literature to derive correctness guarantees for our robust planning framework. Notably, our method boasts several important advantages over existing TMPC approaches, and thus is of independent interest as a novel approach to TMPC. Specifically, due to the difficulty of constructing invariant tubes and associated tracking controllers for nonlinear systems [10], most existing schemes for TMPC for nonlinear systems involve applying methods from linear TMPC by decomposing the dynamics into a linear and a nonlinear component (which is treated as a bounded disturbance) [11], [12]. Other methods rely on Lipschitz bounds, which can often be difficult to obtain [13], [14], or assume the existence of stabilizing tracking controllers [15]. In contrast, our analysis is less conservative since it directly exploits the *intrinsic nonlinear properties* of a system.

Our work is also conceptually related to the notion of incremental input-to-state stability (δ-ISS), which was recently used in [16] for discrete-time systems to characterize invariant tubes as sublevel sets of a δ-ISS Lyapunov function, *assumed* given. δ-ISS has also been studied within a contraction theory framework, e.g., in [17], where contraction metrics are derived for a class of nonlinear systems stabilized using backstepping. In contrast to these methods, our approach allows for both the design *and* optimization of invariant tubes and tracking feedback controllers.

Statement of Contributions: The contribution of this paper is fourfold. First, on the theoretical side, while our CCM approach is directly inspired by [9], we present an alternative proof (Section III) of incremental exponential stability between trajectories using a suitable CCM-derived controller. This proof employs techniques from calculus of variations and differential geometry to (a) derive a tighter characterization of the controller's disturbance rejection properties and the size of the corresponding invariant tube (Section IV-A), and (b) simplify the online implementation of the controller (Section IV-C), under significantly weaker conditions for the CCM as compared to [9] and [17]. Second, we derive a bound on the magnitude of the tracking controller by leveraging properties of CCMs and exploiting analogies with *differential* control Lyapunov functions (Section IV-D). Third, on the algorithmic side, we present an offline/online framework for robust motion planning where in the offline phase, we formulate a quasiconvex optimization problem using SOS programming that searches for an *optimal* CCM in order to minimize the cross-section of the invariant tube (Section IV-B), and derive the structure of a tracking controller that can be efficiently implemented online to minimize control effort. The optimized tube is used online to obtain nominal motion plans that can be robustly tracked (Section II). Fourth, on the experimental front, we illustrate our method on a simulated 6 state planar-quadrotor system (Section VI-A) and also discuss the merits of our approach in comparison with state-of-the-art nonlinear TMPC algorithms (Section VI-B).

Notation: Let $\mathbb{S}_j^+$ and $\mathbb{S}_j$ be the set of symmetric positive definite and semidefinite matrices in $\mathbb{R}^{j\times j}$, respectively. Given a matrix X, let $\widehat{X} := X + X^T$. The set of $\mathcal{C}^2$ functions from $\mathcal{D}$ to $\mathcal{R}$ is denoted by $\mathcal{C}^2(\mathcal{D},\mathcal{R})$. We denote the components of a vector $y \in \mathbb{R}^n$ as $y[j],\ j = 1,\dots,n$, and its Euclidean norm as $\|y\|$. Let $\|y\|_A = \sqrt{y^T A y}$ denote a weighted norm for $A \in \mathbb{S}_n^+$. Let $(\overline{\sigma}(A), \underline{\sigma}(A))$ denote the maximum and minimum singular values of a matrix A and $\partial_y F(x)$ the directional derivative of the matrix valued function F at x along the vector y. Given sets $\mathcal{A}$ and $\mathcal{B}$, the set $\mathcal{A} \ominus \mathcal{B}$ is the Minkowski difference.

II. Problem Formulation

We consider robotic systems whose dynamics are described by the nonlinear differential equation:

$$\dot{x}(t) = f(x(t)) + B(x(t))u(t) + B_w w(t), \qquad (1)$$

where $x(t) \in \mathbb{R}^n$ is the state, $u(t) \in \mathbb{R}^m$ is the control input, and $w(t) \in \mathbb{R}^{n_w}$ is the disturbance. We assume that functions $f(x)$ and $B(x)$ are smooth, and $B_w \in \mathbb{R}^{n\times n_w}$ is a constant matrix with $\bar{\sigma}(B_w) = 1$ (in other words, B_w simply selects the channels where the disturbance is active). We write $B(x)$ in column form as $\big[b_1(x), b_2(x), \dots, b_m(x)\big]$. A state-input trajectory satisfying (1) is denoted as a pair (x, u).

The disturbance signal $w(t)$ is assumed to be piecewise $\mathcal{C}^1$ and norm-bounded, i.e., there exists $\bar{w}$ such that $\|w(t)\| \leq \bar{w}$,

for all $t \geq 0$. We enforce state constraints (e.g., arising from obstacles in the robot's environment and physical constraints such as joint limits) and input constraints, that is: $x(t) \in \mathcal{X}$ and $u(t) \in \mathcal{U}$ for all t, where $\mathcal{X}$ and $\mathcal{U}$ are defined to be the closures of bounded, open, and connected sets in Euclidean space. The motion planning problem we wish to address is to find a (possibly non-stationary) policy $\pi : \mathcal{X} \times \mathbb{R} \to \mathcal{U}$ that (1) drives the state x to a compact region $\mathcal{X}_{\text{goal}} \subseteq \mathcal{X}$, (2) satisfies the state and input constraints, and (3) minimizes a quadratic cost:

$$J(x(t), \pi) := \int_0^{T_{\text{goal}}} 1 + \|\pi(x(t), t)\|_R^2 dt,$$

where $R \in \mathbb{S}_m^+$ and T_{goal} is the first time $x(t)$ enters $\mathcal{X}_{\text{goal}}$. As posed, the motion planning problem entails an optimization over the class of state-feedback functions – a computationally intractable task in general. In an effort to reduce computational complexity, our strategy is to parameterize general state-feedback policies as a sum of a nominal (open-loop) input u^* and a feedback term designed to track the nominal state trajectory x^* (induced by u^* assuming no disturbances):

$$\pi(x(t),\, t) = u^*(t) + k(x^*(t), x(t)). \tag{2}$$

This formulation represents a compromise between the general class of state-feedback control laws and a purely open-loop formulation (i.e., no tracking).

In this work we will assume the existence of a motion planner (e.g., a standard sampling-based planner [18], [19]) that computes a nominal input u^* online (i.e., when obstacles in the environment are reported) in order to drive the initial state to the goal region *assuming no disturbances* while minimizing the quadratic cost. The objective of this paper is to design a tracking feedback controller $k(\cdot, \cdot)$ that can *robustly* track a planned nominal trajectory in the presence of disturbances. Furthermore, we wish to characterize a *robust control invariant (RCI)* tube (defined below) centered around the nominal trajectory that the state of the closed-loop system is guaranteed to remain within when the tracking controller is applied. Consequently, the RCI tube can be used by the motion planner as a robustness margin in order to compute a guaranteed safe nominal motion plan (x^*, u^*) online.

Online synthesis of a tracking controller $k(\cdot, \cdot)$ and associated RCI tube for each nominal motion plan may be prohibitively difficult (see, e.g., [20]). Instead, in this paper we compute both an RCI tube and the structure of a feedback controller *offline* (Section III) and present efficient methods for online implementation of the controller (Section IV). We start with a formal definition of RCI tubes.

A. Robust Control Invariant Tubes

Suppose (x^*, u^*) is a state-input trajectory satisfying the nominal dynamics (i.e., (1) with $w \equiv 0$) and (x, u) is a state-input trajectory satisfying (1) under the action of a parameterized policy (2). Let T^*_{goal} be the first time $x^*(t)$ enters $\mathcal{X}_{\text{goal}}$. An RCI tube is defined as:

Definition II.1 (RCI Tube)**.** *Let $\Omega : \mathbb{R}^n \to 2^{\mathbb{R}^n}$ be a mapping s.t. $x \in \Omega(x)$ and $\Omega(x)$ is a closed and bounded set for every x. Then, $\Omega(\cdot)$ is an RCI mapping (additionally $\Omega(x)$ is an RCI set centered on x) if there exists a tracking controller $k(x^*, x)$ s.t. if $x(t_0) \in \Omega(x^*(t_0))$, then for all allowable realizations of the disturbance $w(t)$, $x(t) \in \Omega(x^*(t))$ for all $t_0 \leq t \leq T^*_{\text{goal}}$. Given an RCI mapping $\Omega(\cdot)$, an RCI tube centered on the trajectory $x^*(t),\ t_0 \leq t \leq T^*_{\text{goal}}$, is the region $\cup_{t_0 \leq t \leq T^*_{\text{goal}}} \Omega(x^*(t))$.*

Intuitively, a tracking controller with an associated RCI tube $\Omega(\cdot)$ guarantees that the state of the system is always "close" to its nominal value $x^*(t)$ (precisely, within set $\Omega(x^*(t))$). In Section IV we will use contraction theory to compute an RCI mapping Ω that is *independent* of the nominal trajectory x^*. Thus, by planning a nominal state-input trajectory satisfying the *tightened* constraints:

$$x^*(\cdot) \in \bar{\mathcal{X}} := \mathcal{X} \ominus \Omega, \tag{3a}$$

$$u^*(\cdot) \in \bar{\mathcal{U}} := \{\bar{u} \in \mathcal{U} : \forall x^*(t) \in \bar{\mathcal{X}}, \forall x(t) \in \mathcal{X} \text{ such that } x(t) \in \Omega(x^*(t)),\, \bar{u} + k(x^*(t), x(t)) \in \mathcal{U}\}, \tag{3b}$$

one can ensure that the robotic system will safely reach the goal region $\mathcal{X}_{\text{goal}}$ (modulo the size of the RCI set) in the presence of disturbances. Note that one can ensure that the system reaches $\mathcal{X}_{\text{goal}}$ (without the extra buffer from the RCI set) by constraining the RCI set to be contained within $\mathcal{X}_{\text{goal}}$ at T^*_{goal}. Constraint (3a) ensures that the RCI tube around the trajectory does not intersect any obstacles, while (3b) is defined for a given tracking controller and ensures that the net applied control satisfies the input limit.

Given such a nominal motion plan (x^*, u^*) defined over the time interval $[0,\, T^*_{\text{goal}}]$, one may adopt two different frameworks for its robust execution. In the first approach, one could simply execute the controller in (2) until the robot enters $\mathcal{X}_{\text{goal}}$. In the second approach, provided there exist sufficient online computational resources, one can use a receding-horizon algorithm in which the nominal trajectory is periodically and *locally* re-updated over a short time-horizon $T < T_{\text{goal}}$. This allows one to reduce the tracking cost (as information about the realized disturbances is taken into account) and is the approach adopted in this paper. Such a receding-horizon strategy is formalized next.

B. Receding Horizon Implementation

Given a robust motion plan (i.e., a nominal state-input trajectory (x^*, u^*) such that the RCI tube centered on x^* does not intersect any obstacles), one can make *local* updates to it using the following MPC problem solved at the discrete time instants $t_i,\ i \in \mathbb{N}_{\geq 0}$:

Optimization Problem MPC — Given current state $x(t_i)$ and a robust motion plan (x^*, u^*) with associated RCI mapping $\Omega(\cdot)$, solve

$$\min_{\substack{\bar{u}(t) \in \mathcal{C}^2([t_i, t_i+T], \bar{\mathcal{U}}) \\ \bar{x}(t_i) \in \bar{\mathcal{X}}}} \int_{t_i}^{t_i+T} \|\bar{u}(\tau)\|_R^2 \, d\tau$$

subject to

$$x(t_i) \in \Omega(\bar{x}(t_i)), \tag{4}$$

$$\dot{\bar{x}}(\tau) = f(\bar{x}(\tau)) \ + B(\bar{x}(\tau))\bar{u}(\tau), \tag{5}$$

$$\bar{x}(\tau) \in \bar{\mathcal{X}}, \qquad \bar{u}(\tau) \in \bar{\mathcal{U}},\ \forall \tau \in [t_i, t_i + T] \tag{6}$$

$$\bar{x}(t_i + T) = \qquad x^*(t_i + T). \tag{7}$$

Problem MPC should be understood as a *local* re-optimization step – thus it should be solved using *local* methods such as trajectory optimization techniques [21] or elastic bands [22] (as opposed to fully-fledged global planners). Notice that the initial value of the updated nominal state trajectory, i.e., $\bar{x}(t_i)$, is also an optimization variable above subject to the RCI constraint (4). This permits more drastic updates to the nominal trajectory, e.g., to counteract consistently large disturbances. The terminal constraint given by (7) is used to ensure *recursive feasibility* for the MPC problem, as addressed by the next lemma. The state-input pair solution to problem MPC is denoted as $(x_T^*(t;\bar{x}(t_i)), u_T^*(t;\bar{x}(t_i))) : [t_i, t_i+T] \to \bar{\mathcal{X}} \times \bar{\mathcal{U}}$, of which the segment $[t_i, t_i+\delta)$ is implemented using (2), before MPC is re-solved (with $\delta < T$). This defines the *sampled* MPC strategy commonly employed for continuous-time systems. The following lemma establishes recursive feasibility for problem MPC.

Lemma II.2 (Recursive Feasibility for MPC)**.** *Suppose problem MPC is feasible at the initial solve step $t_0 = 0$. Then, the problem is feasible for all $t_i, i \in \mathbb{N}_{\geq 0}$.*

Proof. Let $(x_T^*(t;\bar{x}(t_i)), u_T^*(t;\bar{x}(t_i))) : [t_i, t_i+T] \to \bar{\mathcal{X}} \times \bar{\mathcal{U}}$ denote the solution to problem MPC at time-step t_i. Then at solve time $t_{i+1} = t_i + \delta$, due to the RCI property associated with the tracking controller, one is guaranteed that the actual state $x(t_i)$ lies within the set $\Omega(x_T^*(t_{i+1};\bar{x}(t_i)))$. Consider then the following feasible, but possibly suboptimal solution to problem MPC at solve time t_{i+1}:

$$\bar{x}(\tau) = \begin{cases} x_T^*(\tau;\bar{x}(t_i)) & \text{for } \tau \in [t_{i+1}, t_i+T] \\ x^*(\tau) & \text{for } \tau \in [t_i+T, t_{i+1}+T], \end{cases}$$

$$\bar{u}(\tau) = \begin{cases} u_T^*(\tau;\bar{x}(t_i)) & \text{for } \tau \in [t_{i+1}, t_i+T] \\ u^*(\tau) & \text{for } \tau \in [t_i+T, t_{i+1}+T], \end{cases}$$

The state-input trajectory above is simply a concatenation of the tail portion of the previous solution with the nominal motion plan solution, and represents a feasible solution for problem MPC due to the terminal constraint (7) (which guarantees that $x_T^*(\cdot,\bar{x}(t_i))$ rejoins the nominal motion plan x^* at time $t_i + T$). Hence, the feasible set of the MPC problem at solve time t_{i+1} is not empty, which proves recursive feasibility. □

C. Overall Algorithm

Algorithm 1 provides pseudocode for our overall approach.

Algorithm 1 Robust planning algorithm

OFFLINE:
Inputs: dynamics model, $\mathcal{U}$ (control input constraints)
Compute: Ω (RCI set), $k(\cdot,\cdot)$ (controller structure)
ONLINE:
Inputs: $x(0)$ (initial state), $\mathcal{X}$ (state constraints), $\mathcal{X}_{\text{goal}}$
Compute nominal (x^*, u^*), such that $x^*(\cdot) \in \overline{\mathcal{X}}$
Initialize: $t_{\text{plan}} \leftarrow 0$
At each time t:
if New obstacles reported or goal region is changed **then**
  Re-plan nominal (x^*, u^*)
else if $t - t_{\text{plan}} = \delta$ **then**
  $(x_T^*(\cdot;\bar{x}(t)), u_T^*(\cdot;\bar{x}(t))) \leftarrow \text{MPC}(x(t), x^*, u^*, \Omega)$
  Update $t_{\text{plan}} \leftarrow t$
end if
Apply control $u_T^*(t;\bar{x}(t_{\text{plan}})) + k(x_T^*(t;\bar{x}(t_{\text{plan}}), x(t))$

III. Control Contraction Metrics and Differential Controllers

In this section we define incremental exponential stability as the measure of convergence between trajectories used in this paper (Section III-A), formally introduce control contraction metrics as *differential* analogues of control Lyapunov functions (Section III-B), and define the notion of a *differential* controller which when integrated, yields an exponentially stabilizing tracking feedback controller (Section III-C). Note that all state-input trajectories in this section are assumed to be solutions to the nominal dynamics (i.e., with $w \equiv 0$).

A. Incremental Exponential Stability

Definition III.1 (Incremental Exponential Stability)**.** *Consider a nominal state-input trajectory pair $(x^*(t), u^*(t))$. Suppose there exist $\lambda, C > 0$ and a controller of the form $u^*(t) + k(x^*(t), x(t))$ such that*

$$\|x^*(t) - x(t)\| \leq Ce^{-\lambda t}\|x^*(0) - x(0)\|, \tag{8}$$

where $(x(t), u^*(t) + k(x^*(t), x(t)))$ is a state-input solution trajectory for the nominal dynamics. Then, the trajectory $x^*(t)$ is said to be incrementally exponentially stabilizable (IES) with rate λ and overshoot constant C.

B. Control Contraction Metrics

Denote the tangent space of $\mathcal{X}$ at $x \in \mathcal{X}$ by $T_x\mathcal{X}$[1] and the tangent bundle of $\mathcal{X}$ by $T\mathcal{X} = \bigcup_{x\in\mathcal{X}}\{x\} \times T_x\mathcal{X}$. The variational dynamics [9] (i.e., dynamics characterizing infinitesimal displacements with respect to a nominal trajectory) for the nominal system are defined as

$$\dot{\delta}_x = \overbrace{\left(\frac{\partial f(x)}{\partial x} + \sum_{j=1}^{m} u[j]\frac{\partial b_j(x)}{\partial x}\right)}^{:=A(x,u)} \delta_x + B(x)\delta_u, \tag{9}$$

where $\delta_x \in T_x\mathcal{X}$ is a tangent vector to a smooth path of states at $x \in \mathcal{X}$, and $\delta_u \in T_u\mathcal{U}$ is a tangent vector to a smooth path of controls at $u \in \mathcal{U}$. Let $M : \mathbb{R}^n \to \mathbb{S}_n^+$ be a smooth matrix function that is uniformly bounded (i.e., there exist constants $0 < \underline{\alpha} < \overline{\alpha}$ such that $\underline{\alpha} I_n \preceq M(x) \preceq \overline{\alpha} I_n$). The inner product $V(x, \delta_x) := \delta_x^T M(x)\delta_x$ endows $\mathcal{X}$ with a Riemannian metric according to the metric tensor $M(x)$, and represents an infinitesimal measure of length on $\mathcal{X}$. For a given smooth curve $c : [0,1] \to \mathcal{X}$, we define its length $l(c)$ and energy $\mathcal{E}(c)$ as $l(c) := \int_0^1 \sqrt{V(c(s), c_s(s))}ds$, $\mathcal{E}(c) := \int_0^1 V(c(s), c_s(s))ds$, where $c_s(s) = \partial c(s)/\partial s$.

Let $\Gamma(p, q)$ be the set of smooth curves on $\mathcal{X}$ that connect points p and q. Define $d(p, q) := \inf_{c\in\Gamma(p,q)} l(c)$ and let $\gamma \in \Gamma(p, q)$ be the (possibly non-unique) *minimizing geodesic* which achieves this infimum. Note that $d^2(p, q) = \mathcal{E}(\gamma)$.

[1]Since $\mathcal{X}$ is simply the closure of an open set in $\mathbb{R}^n$, the tangent space $T_x\mathcal{X}$ for all x in the interior of $\mathcal{X}$ is simply $\mathbb{R}^n$ while $T_x\mathcal{X}$ on the boundary is a half-space in $\mathbb{R}^n$.

A control contraction metric (CCM) on $\mathcal{X}$ is a covariant 2-tensor field $M(x)$ such that the induced Riemannian metric $V(x,\delta_x)$ shrinks at all points in $T\mathcal{X}$, i.e., there exists a *differential* controller $\delta_u : T\mathcal{X} \to T_u\mathcal{U}$, such that $\dot{V}(x,\delta_x) < 0,\ \forall (x,\delta_x) \in T\mathcal{X}$. Thus, $V(x,\delta_x)$ may be interpreted as a *differential* control Lyapunov function (CLF) on the tangent bundle $T\mathcal{X}$ – extending an analogy also explored in [23] using Finsler metrics, albeit, for *closed-loop* systems. Suppose now that the following two conditions hold for some constant $\lambda > 0$ and all $(x,\delta_x) \in T\mathcal{X}$:

$$\partial_{b_j} M(x) + \widehat{M(x)\frac{\partial b_j(x)}{\partial x}} = 0, \qquad j = 1,\dots,m \tag{10}$$

$$\delta_x^T \left(\partial_f M(x) + \widehat{M(x)\frac{\partial f(x)}{\partial x}} \right) \delta_x < -2\lambda \delta_x^T M(x) \delta_x \tag{11}$$

$$\text{for all } \delta_x \text{ such that } \delta_x^T M(x) B(x) = 0.$$

Condition (10) implies that the vectors b_j form a Killing vector field for the metric tensor $M(x)$, while (11) indicates that for all directions where the system lacks controllability (given by the nullspace of $B^T(x)M(x)$), the system is naturally contracting with rate λ. Under conditions (10) and (11), $\dot{V}$ reduces to:

$$\begin{aligned}\dot{V}(x,\delta_x,\delta_u) =& \delta_x^T \left(\widehat{M(x)\frac{\partial f(x)}{\partial x}} \right) \delta_x + 2\delta_x^T M(x) B(x) \delta_u \\ &+ \delta_x^T \left(\partial_f M(x) \right) \delta_x.\end{aligned} \tag{12}$$

C. Incrementally Stabilizing Controllers

Given conditions (10) and (11), [9] shows that there always exists an integrable *differential* feedback controller of the form $\delta_u(x,\delta_x) = K(x)\delta_x$ such that the following inequality holds for all $(x,\delta_x) \in \mathcal{X} \times \mathbb{R}^n$ [2]:

$$\begin{aligned}\dot{V}(x,\delta_x) &= \delta_x^T \left(\partial_f M(x) + \widehat{M(x)\frac{\partial f(x)}{\partial x}} + \widehat{M(x)B(x)K(x)} \right) \delta_x \\ &< -2\lambda \delta_x^T M(x) \delta_x = -2\lambda V(x,\delta_x).\end{aligned} \tag{13}$$

In the scenario where (10) fails to be true, one may leverage the following weaker alternative to conditions (10) and (11):

$$\delta_x^T \left(\partial_{f+Bu} M(x) + \widehat{M(x)A(x,u)} \right) \delta_x < -2\lambda \delta_x^T M(x) \delta_x \tag{14}$$

$$\text{for all } \delta_x \text{ such that } \delta_x^T M(x) B(x) = 0.$$

In [9], it is proven, by construction, that the weaker condition above is still sufficient to guarantee the existence of a differential feedback controller, however, the differential controller is now a function of u as well, i.e., $\delta_u = \delta_u(x,\delta_x,u)$. Given a desired nominal state-input trajectory pair $(x^*(t),u^*(t))$, let $\gamma(\cdot,t) \in \Gamma(x^*(t),x(t))$ denote a minimizing geodesic connecting $x^*(t)$ and $x(t)$. Consider the following control law:

$$\begin{aligned}\pi(x(t),t) &= u^*(t) + \int_{\gamma(\cdot,t)} \delta_u(\gamma(s,t),\delta_\gamma(s,t))ds \\ &= u^*(t) + \underbrace{\int_0^1 K(\gamma(s,t))\delta_\gamma(s,t)ds}_{=k(x^*(t),x(t))},\end{aligned} \tag{15}$$

where $\delta_\gamma(s,t) := \partial\gamma(s,t)/\partial s$. The geometric interpretation of (15) and inequality (13) is illustrated in Fig. 2. In case the weaker condition (14) is used, $\delta_u = \delta_u(x,\delta_x,u)$, and thus $\pi(x(t),t)$ will be given by the solution to the differential equation

$$\pi(x(t),t) = u^*(t) + \int_{\gamma(\cdot,t)} \delta_u(\gamma(s,t),\delta_\gamma(s,t),\pi(\gamma(s,t),t))ds, \tag{16}$$

where $\delta_u(\cdot)$ is designed such that $\dot{V}(x,\delta_x,u)$ is less than $-2\lambda V(x,\delta_x)$ for all (x,δ_x) along the minimizing geodesic. Theorem III.2, which is central to our approach, proves that control law (15) ensures the trajectory $x(t)$ is IES with respect to $x^*(t)$ in the sense of Definition III.1. The proof differs significantly from the one presented in [9] as it is later adapted in the next section for deriving the RCI mapping.

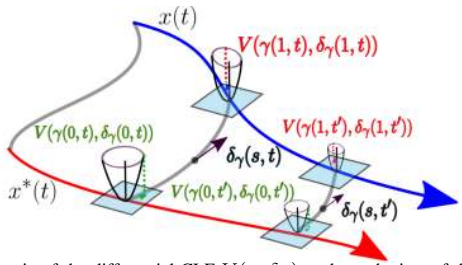

Fig. 2: Schematic of the differential CLF $V(x,\delta x)$ at the endpoints of the geodesics $\gamma(\cdot,t)$ and $\gamma(\cdot,t')$ at times t and $t' > t$ and the geodesic velocity vector at the position $s \in (0,1)$ along the geodesic. The contours of V are shaped according to the metric tensor $M(x)$. The differential controller ensures that at all points along the geodesic, $V(x,\delta_x)$ is shrinking in the direction tangent to the geodesic.

Theorem III.2 (Incrementally stabilizing controller)**.** *Let (x^*,u^*) and (x,u) be state-input trajectory pairs for the nominal dynamics where $\pi(x(t),t)$ is given by* (15) *using a CCM which satisfies equations* (10) *and* (11) [3] *. Then, $x(t)$ is IES with respect to $x^*(t)$ in the sense of Definition III.1.*

Proof. We give the proof for a CCM satisfying the stronger condition in (10) since the corresponding argument for the weaker condition is identical with only minor adjustments. Let ϵ be a small positive constant. At time $t' \geq 0$, construct a parameterized *surface* of solutions $c : [0,1] \times (t'-\epsilon, t'+\epsilon) \to \mathcal{X}$ to the nominal dynamics subject to the following version of the control law (15):

$$\pi(c(s,t),t) = u^*(t) + \int_0^s \delta_u(c(\mathfrak{s},t),\delta_c(\mathfrak{s},t))d\mathfrak{s}, \tag{17}$$

where the integral above is computed along the curve $c(\cdot,t)$ and $c(\cdot,t') = \gamma(\cdot,t')$, the minimizing geodesic at time t'. Notice that the curve $t \to c(0,t)$ corresponds to the trajectory $x^*(t)$ for $t \in (t'-\epsilon, t'+\epsilon)$ while the curve $t \to c(1,t)$ is an osculating curve to the trajectory $x(t)$ at $t = t'$ since $c(\cdot,t') = \gamma(\cdot,t')$ and thus, $\pi(c(1,t'),t') = \pi(x(t'),t)$. This is illustrated in Fig. 3.

Consider the time derivative of the Riemann energy $\mathcal{E}(c(\cdot,t))$ of the parameterized solutions:

$$\dot{\mathcal{E}}(c(\cdot,t)) = \int_0^1 \frac{\partial V(s,t)}{\partial t} ds, \tag{18}$$

[2]Note that we drop the distinction between $T_x\mathcal{X}$ at the boundary versus the interior and simply assume that $T_x\mathcal{X} = \mathbb{R}^n$.

[3]Alternatively, $\pi(x(t),t)$ is given by (16) using a CCM satisfying the weaker condition (14).

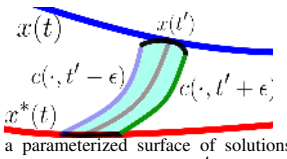

Fig. 3: Construction of a parameterized surface of solutions $c(\cdot,\cdot)$ (shaded blue) anchored at the geodesic (shown in grey) at time t'. The path endpoint $t \to c(0,t)$ coincides with $x^*(t)$ and $t \to c(1,t)$ is an osculating curve at $x(t')$.

where we have employed the shorthand $V(s,t) = V(c(s,t), \delta_c(s,t))$. Then, by application of the control law in (15) along with inequality (13), one has that $\dot{V}(s,t) \leq -2\lambda V(s,t)$ for all $s \in [0,1]$ and $t \in (t'-\epsilon, t'+\epsilon)$. It follows that $\dot{\mathcal{E}}(c(\cdot,t))\Big|_{t=t'} \leq -2\lambda \mathcal{E}(c(\cdot,t'))$. We now further manipulate (18) as follows:

$$\dot{\mathcal{E}}(c(\cdot,t)) = \int_0^1 \left[\left(\frac{\partial V(s,t)}{\partial c(s,t)} \right)^T \frac{\partial c(s,t)}{\partial t} + \left(\frac{\partial V(s,t)}{\partial \delta_c} \right)^T \frac{\partial \delta_c(s,t)}{\partial t} \right] ds \tag{19}$$

Recall that $\delta_c(s,t) = \partial c(s,t)/\partial s$. Thus, we may write

$$\frac{\partial \delta_c(s,t)}{\partial t} = \frac{\partial^2 c(s,t)}{\partial t \partial s} = \frac{\partial^2 c(s,t)}{\partial s \partial t},$$

where the order of differentiation can be swapped since $c(\cdot,\cdot) \in \mathcal{C}^2$. Substituting the expression above back into (19) and using integration-by-parts yields

$$\dot{\mathcal{E}}(c(\cdot,t)) = \int_0^1 \left(\frac{\partial V(s,t)}{\partial c(s,t)} - \frac{\partial}{\partial s}\left(\frac{\partial V(s,t)}{\partial \delta_c} \right) \right)^T \frac{\partial c(s,t)}{\partial t} ds + \left[\left(\frac{\partial V(s,t)}{\partial \delta_c} \right)^T \frac{\partial c(s,t)}{\partial t} \right] \Bigg|_{s=0}^{s=1},$$

Notice that at time $t = t'$, $c(\cdot,t')$ is *the* minimizing geodesic. Thus, the bracketed expression in the integrand above is 0 for all $s \in [0,1]$ since $c(\cdot,t')$ must necessarily satisfy the Euler-Lagrange equation. Thus, at time $t = t'$, we have:

$$\dot{\mathcal{E}}(c(\cdot,t))\Big|_{t=t'} = \left[\left(\frac{\partial V(s,t)}{\partial \delta_c} \right)^T \frac{\partial c(s,t)}{\partial t} \right] \Bigg|_{s=0,\ t=t'}^{s=1}. \tag{20}$$

Consider the time derivative of the Riemann energy of the minimizing geodesic between $x^*(t)$ and $x(t)$. If $x(t') \notin \text{Cut}(x^*(t'))$ (where $\text{Cut}(x)$ denotes the cut-locus at x), then the derivative of $\mathcal{E}(\gamma(\cdot,t))$ is well-defined at $t = t'$ (i.e., the exponential map is a local diffeomorphism) and given by [24, Chp 9]:

$$\dot{\mathcal{E}}(\gamma(\cdot,t)\Big|_{t=t'} = \left[\left(\frac{\partial V(s,t)}{\partial \delta_\gamma} \right)^T \frac{\partial \gamma(s,t)}{\partial t} \right] \Bigg|_{s=0,t=t'}^{s=1}. \tag{21}$$

Notice that since $c(\cdot,t') = \gamma(\cdot,t')$, the expression above and the one in (20) must be equal at $t = t'$. Thus, we arrive at the following chain of inequalities:

$$\dot{\mathcal{E}}(\gamma(\cdot,t)\Big|_{t=t'} = \dot{\mathcal{E}}(c(\cdot,t))\Big|_{t=t'} \leq -2\lambda \mathcal{E}(c(\cdot,t')) = -2\lambda \mathcal{E}(\gamma(\cdot,t')).$$

This result is true for all $t' \geq 0$ such that $x(t') \notin \text{Cut}(x^*(t'))$. For completeness, suppose now that $x(t') \in \text{Cut}(x^*(t'))$, a Lebesgue measure zero set. In this scenario, the minimizing geodesic $\gamma(\cdot,t')$ may not be unique and thus the Riemannian distance $d(x^*(t), x(t))$ is *not* smooth at $t = t'$. However, it can be shown that the upper Dini derivative of $\mathcal{E}(\gamma(\cdot,t))$ defined as:

$$D^+\mathcal{E}(\gamma(\cdot,t))\big|_{t=t'} = \limsup_{t \searrow t'} \frac{\mathcal{E}(\gamma(\cdot,t)) - \mathcal{E}(\gamma(\cdot,t'))}{t - t'}$$

exists and satisfies the inequality [25][4]

$$D^+\mathcal{E}(\gamma(\cdot,t)\big|_{t=t'} \leq \left[\left(\frac{\partial V(s,t)}{\partial \delta_\gamma} \right)^T \frac{\partial \gamma(s,t)}{\partial t} \right] \Bigg|_{s=0,t=t'}^{s=1}, \tag{22}$$

where D^+ denotes the upper right Dini derivative. The rest of the proof proceeds as before, yielding the following inequalities:

$$D^+\mathcal{E}(\gamma(\cdot,t)\big|_{t=t'} \leq \dot{\mathcal{E}}(c(\cdot,t))\Big|_{t=t'} \leq -2\lambda \mathcal{E}(c(\cdot,t')) = -2\lambda \mathcal{E}(\gamma(\cdot,t')), \tag{23}$$

for all $t' \geq 0$. By the Comparison Lemma [26], $\mathcal{E}(\gamma(\cdot,t)) \leq \mathcal{E}(\gamma(\cdot,0))e^{-2\lambda t}$. Since $d^2(x^*(t),x(t)) = \mathcal{E}(\gamma(\cdot,t))$ and the metric tensor $M(x)$ is uniformly bounded, one concludes

$$\|x(t) - x^*(t)\| \leq \sqrt{\frac{\overline{\alpha}}{\underline{\alpha}}} \|x(0) - x^*(0)\| e^{-\lambda t}.$$

Thus, $x^*(t)$ is IES with rate λ and overshoot $\sqrt{\overline{\alpha}/\underline{\alpha}}$. □

The construction of the surface of solutions is needed as one *cannot* directly reason about the evolution of the minimizing geodesic, i.e., $c(s,t) \neq \gamma(s,t)$ for $s \in (0,1)$ except at $t = t'$. Instead, we leverage the Euler-Lagrange equation to relate the time derivative of the Riemann energy of the surface of solutions with that of the minimizing geodesic. Thus, the energy of the minimizing geodesic may be viewed as an *incremental* CLF, thereby defining the structure of the feedback controller as a smooth function that needs to satisfy inequality (23). The key idea of this paper is to use the tracking controller $k(\cdot,\cdot)$ to yield the invariant tube and accompanying robustness guarantees.

While the interpretation of the energy as an incremental CLF is an observation also made in [9], by showing equivalence between the right hand sides of (18), (20), and (21) and using this to establish IES for $x^*(t)$, we are able to derive the robustness guarantees for controller (15) under significantly weaker conditions than those necessary in [9]. We explore this distinction in greater detail in Section IV-A.

Remark III.3. *It can be shown that conditions* (10) *and* (11) *are* invariant *under state diffeomorphism and metric pushforward [9]. This invariance allows one to relax the topological assumptions on the state space $\mathcal{X}$. In particular, one may take $\mathcal{X}$ to be an embedded $n-$manifold in $\mathbb{R}^k$ where $k \geq n$, as long as the contraction conditions hold on one (and thus, any) choice of local coordinates in $\mathbb{R}^n$. This highlights the coordinate-free (i.e., intrinsic) nature of CCM-based stabilization.*

IV. Contraction-Based Tubes and Controllers

In this section we: (1) derive the RCI mapping for a *given* tracking feedback controller using contraction-theoretical tools (Section IV-A), (2) show how to compute CCMs that

[4]In actual fact, it is shown in [25] that the one-sided derivative of $\mathcal{E}(\gamma(\cdot,t))$ along any tangent vectors at $x^*(t')$ and $x(t')$ (defined using $\lim_{t \searrow t'}(\cdot)$) exists from which it follows that the limit $\limsup_{t \searrow t'}(\cdot)$ exists.

minimize a certain measure of the size of the RCI set (Section IV-B), (3) propose an offline/online approach where a CCM is computed offline and the tracking controller is implemented online by using the CLF analogy introduced in the previous section (Section IV-C), and (4) derive a bound on the tracking control effort allowing us to compute the tightened control constraint set $\bar{\mathcal{U}}$ (Section IV-D). Henceforth, $(x^*(t), u^*(t))$ is assumed to satisfy the nominal dynamics, while $x(t)$ denotes the actual state trajectory (i.e., with disturbances) using the control law $u^*(t) + k(x^*, x)$, where $k(x^*, x)$ is a CCM-derived tracking controller.

A. Feasible Contraction-Based Tubes

In this section we derive the RCI mapping assuming that the feedback controller is given by (15) using a CCM.

Theorem IV.1 (Disturbance Rejection)**.** *Assume there exists a CCM $M(x)$ satisfying conditions* (10) *and* (11) *that is uniformly bounded, i.e., $\underline{\alpha} I_n \preceq M(x) \preceq \overline{\alpha} I_n$, for all $x \in \mathcal{X}$ where $\underline{\alpha} > 0$. Factorize $M(x)$ as $\Theta(x)^T \Theta(x)$ and define $\overline{\alpha}_w := \overline{\sigma}(\Theta(x) B_w)$. Then, the geodesic energy between trajectories $x(t)$ and $x^*(t)$, i.e., $\mathcal{E}(\gamma(\cdot, t))$, satisfies the differential inequality:*

$$D^+\mathcal{E}(\gamma(\cdot,t)) \leq -2\lambda \mathcal{E}(\gamma(\cdot,t)) + 2d(x^*(t), x(t))\overline{\alpha}_w \|w(t)\|. \quad (24)$$

Proof. Inequality (22) implies:

$$\begin{aligned} D^+\mathcal{E}(\gamma(\cdot,t)) \leq\ & 2\delta_\gamma^T(1,t) M(\gamma(1,t)) (f(x(t)) + B(x(t))u(x(t)) \\ & - 2\delta_\gamma^T(0,t) M(\gamma(0,t)) \left(f(x^*(t)) + B(x^*(t))u^*(t)\right) \\ & + 2\delta_\gamma^T(1,t) M(\gamma(1,t)) B_w w(t)), \end{aligned} \quad (25)$$

where $u(x(t))$ is given by (15). By the IES property of the nominal system, i.e., inequality (23), the expression above can be bounded as:

$$D^+\mathcal{E}(\gamma(\cdot,t)) \leq -2\lambda \mathcal{E}(\gamma(\cdot,t)) + 2\delta_\gamma^T(1,t) M(\gamma(1,t)) B_w w(t).$$

Defining $\delta_z(s,t) := \Theta(\gamma(s,t))\delta_\gamma(s,t)$, we obtain

$$D^+\mathcal{E}(\gamma(\cdot,t)) \leq -2\lambda \mathcal{E}(\gamma(\cdot,t)) + 2\delta_z^T(1,t) \Theta(\gamma(1,t)) B_w w(t).$$

Recall that the velocity field of a geodesic is *parallel* along the geodesic [24] and thus $V(\gamma(s,t), \delta_\gamma(s,t)) = \mathcal{E}(\gamma(\cdot,t))$ for all $s \in [0,1]$. This implies that $\sqrt{V(\gamma(s,t), \delta_\gamma(s,t))} = \|\delta_z(s,t)\| = d(x^*(t), x(t))$. Using the Cauchy-Schwarz inequality one obtains the stated differential inequality. □

Remark IV.2. *Notice that the differential inequality derived in* (24) *may be integrated in time to yield a $\delta-ISS$ statement similar to Definition 2.3 in [17]. Specifically, in [17], the authors prove $\delta - ISS$ by leveraging a decrescent condition similar to inequality* (13) *with respect to tangent vectors δ_w defined on the tangent space of the disturbance manifold $\mathcal{W}$, yielding a* differential *ISS condition. The key difference here then is by leveraging the separability of the disturbance term (i.e., inequality* (25)*), and by using a tracking controller that enforces contraction along the minimizing geodesic at each time (see Fig. 2), we* do not *need to impose similar differential ISS like conditions on $V(x, \delta_x)$. We further note that a similar bound is also proved in [9] but under stronger conditions, which resemble the differential ISS conditions in [17]. Indeed, the relaxation of such conditions for Theorem IV.1 is the primary motivation for our alternative proof strategy for Theorem III.2.*

Since $\|w(t)\| \leq \bar{w}$ for all t, and the right-hand side of (24) is locally Lipschitz in $\mathcal{E}$ (for $\mathcal{E} > 0$), then if $d(x^*(0), x(0)) \in (0, \overline{\alpha}_w \bar{w}/\lambda]$, by the Comparison Lemma [26], the geodesic distance is upper bounded by $\overline{\alpha}_w \bar{w}/\lambda$, for all time $t \geq 0$. Thus, the RCI mapping may be expressed as:

$$\Omega(x^*) = \{x \in \mathcal{X} : d(x^*, x) \leq \overline{\alpha}_w \bar{w}/\lambda := \bar{d}\}, \quad (26)$$

and will be implemented within the initial state constraint (4) in problem MPC. Notice that the mapping above is given using the Riemann distance which may depend on a spatially varying metric. In order to efficiently plan a nominal trajectory whose associated RCI tube doesn't collide with obstacles, we would prefer a mapping that is *independent* of x^*. To this end, consider the following technical lemma.

Lemma IV.3. *(Geodesic Boundedness) Consider points $x^* \in \bar{\mathcal{X}}, x \in \mathcal{X}$ s.t. $x \in \Omega(x^*)$ where $\Omega(x^*)$ is given in* (26)*. Suppose the CCM $M(x)$ satisfies $M(x) \succeq \underline{M}$ for all $x \in \mathcal{X}$, where $\underline{M} \succeq \underline{\alpha} I_n$. Define the ellipsoid*

$$\widetilde{\Omega}(x^*) := \{x \in \mathcal{X} : \|x - x^*\|^2_{\underline{M}} \leq \bar{d}^2\}, \quad (27)$$

and suppose $\widetilde{\Omega}(x^*) \subset \mathcal{X}$. Then, the minimizing geodesic γ is contained entirely within $\widetilde{\Omega}(x^*)$, i.e., $\gamma(s) \in \widetilde{\Omega}(x^*)$ for all $s \in [0,1]$, and thus $\Omega(x^*) \subseteq \widetilde{\Omega}(x^*)$.

Proof. Consider the following chain of inequalities:

$$\begin{aligned} \mathcal{E}(\gamma) &= \int_0^1 \delta_\gamma(s)^T M(\gamma(s)) \delta_\gamma(s) ds \\ &\geq \int_0^1 \delta_\gamma(s)^T \underline{M} \delta_\gamma(s) ds \\ &\geq \|x - x^*\|^2_{\underline{M}}, \end{aligned}$$

where the first inequality follows from the Lemma condition, and the second inequality follows from the fact that $\underline{M} \in \mathbb{S}^+_n$ defines a flat Riemannian metric under which geodesics are straight lines. Thus, we obtain the implication:

$$\mathcal{E}(\gamma) \leq \bar{d}^2 \Rightarrow \|x - x^*\|^2_{\underline{M}} \leq \bar{d}^2.$$

To complete the proof we note that since γ is a minimizing geodesic, it follows that $d(x^*, \gamma(s)) = s d(x^*, x)$ for all $s \in [0,1]$. □

Equation (27) gives an ellipsoidal outer approximation of the RCI tube as defined in (26), and is thus independent of x^*. This is essential for two reasons: (1) it drastically simplifies collision checking with respect to obstacles by avoiding geodesic computations, and (2) the tightened state constraint set $\bar{\mathcal{X}}$ in problem MPC must be taken to be $\mathcal{X} \ominus \widetilde{\Omega}$ to ensure that the minimizing geodesic lies within $\mathcal{X}$, i.e., where the CCM conditions hold.

We next show how one can leverage convex optimization and SOS programming to compute an *optimized* CCM that minimizes the size of the RCI tube and the outer ellipsoidal approximation. This in turn minimizes the deviation of the perturbed trajectory from the nominal, thereby reducing the amount by which we must tighten the set $\mathcal{X}$.

B. Optimized Contraction-Based Tubes

As shown in [9], condition (11) can be written as a pointwise Linear-Matrix-Inequality (LMI) by introducing the

dual metric $W(x) := M(x)^{-1}$ and the change of variables $\eta_x := M(x)\delta_x$. Specifically, define a matrix $B_\perp(x)$ whose columns form a basis for the null space of $B(x)^T$ (i.e., $B(x)^T B_\perp(x) = 0$). Then, conditions (10) and (11) are equivalent to:

$$\partial_{b_j} W(x) - \widehat{\frac{\partial b_j(x)}{\partial x} W(x)} = 0, \quad j = 1, \dots, m \tag{28}$$

$$B_\perp^T \left(-\partial_f W(x) + \widehat{\frac{\partial f(x)}{\partial x} W(x)} + 2\lambda W(x) \right) B_\perp \prec 0. \tag{29}$$

The equivalent reformulation of the weaker condition (14) in terms of the dual metric is given by LMI (29) and:

$$B_\perp^T \left(\partial_{b_j} W(x) - \widehat{\frac{\partial b_j(x)}{\partial x} W(x)} \right) B_\perp = 0, \ j = 1, \dots, m. \tag{30}$$

In this section we replace the CCM *feasibility* problem, i.e., conditions (28) and (29), with a quasiconvex optimization problem to minimize the size of the outer approximation for the RCI mapping. A trade-off between the overshoot constant $\sqrt{\overline{\alpha}/\underline{\alpha}}$ and contraction rate λ was briefly discussed in [27]. Here, we further explore this aspect by formulating a global *optimization* program to characterize such a trade-off and minimize conservatism. Ideally, one would directly like to minimize the bound in (27) subject to conditions (28) and (29). However, this problem is non-convex and infinite-dimensional. Hence, we consider a tractable, finite-dimensional, quasiconvex approximation whereby the dual metric $W(x)$ is parameterized as a matrix polynomial and the LMIs are written as SOS constraints, enforced over the semi-algebraic set $\mathcal{X}$ using the Positivstellensatz relaxations [28]. Recognizing that for a fixed contraction rate λ, the CCM conditions define a convex feasibility region for $W(x)$, consider the problem $\mathcal{OPT}_{\widehat{CCM}}$:

Optimization Problem $\mathcal{OPT}_{\widehat{CCM}}$ — Solve

$$\min_{\lambda \in \mathbb{R}_{>0}} \ \min_{\substack{W \in \mathcal{C}^\infty(\mathcal{X}, \mathbb{S}_n^+) \\ \overline{W} \in \mathbb{S}_n^+, \ \underline{\beta}, \overline{\beta} \in \mathbb{R}_{>0}}} \quad J_{CCM}(\underline{\beta}, \overline{\beta}, \lambda) := \frac{1}{\lambda^2} \left(\overline{\beta} / \underline{\beta} \right)$$

$$\text{subject to} \quad \text{eq. (28), eq. (29)} \tag{31}$$

$$\underline{\beta} I_n \preceq W(x) \preceq \overline{W} \preceq \overline{\beta} I_n \tag{32}$$

where the conditions hold uniformly for all $x \in \mathcal{X}$.

The objective function J_{CCM} is an upper-bound on the *worst-case* (normalized) Euclidean distance within the ellipsoid defined in (27) since from (32), we have: $\overline{\alpha} = 1/\underline{\beta}$, $\underline{\alpha} = 1/\overline{\beta}$, and $\underline{M} = \overline{W}^{-1}$. Thus,

$$\sup_{x \in \widetilde{\Omega}(x^*)} \frac{\|x - x^*\|^2}{\bar{w}^2} = \frac{\overline{\alpha}_w^2}{\lambda^2 \underline{\alpha}} \leq \frac{1}{\lambda^2} \left(\frac{\overline{\alpha}}{\underline{\alpha}} \right) = J_{CCM}.$$

Minimizing the condition number of a positive definite matrix over a closed convex set is quasiconvex [29] and may be solved using a sequence of convex feasibility problems. In this paper, we leverage an additional cost function within the feasibility problems, namely, minimization of $\text{tr}(W_s^T \overline{W} W_s)$ where $\text{tr}(\cdot)$ denotes the trace. The matrix $W_s \in \mathbb{S}_n^+$ is a scaling matrix chosen to shape the ellipsoid $\widetilde{\Omega}(\cdot)$ to minimize its projection on more stringently constrained states. Problem $\mathcal{OPT}_{\widehat{CCM}}$ can then be solved using line search on λ, where for a fixed λ one has to solve a sequence of SOS programs.

The solution to problem $\mathcal{OPT}_{\widehat{CCM}}$ provides an optimized CCM and an RCI tube, computed *offline*. In the next section we use the computed CCM to formulate the online implementation of the feedback controller.

C. Offline/Online Tracking Control via Contraction Theory

By minimizing the tracking control effort, one can curtail the suboptimality introduced by the parameterization (2). Given a CCM computed offline by solving problem $\mathcal{OPT}_{\widehat{CCM}}$, the feedback controller is computed as a solution to the following QP:

Optimization Problem $\mathcal{OPT}_{\textbf{online}}$ — At time $t \geq 0$, given a desired/current state pair $(x^*(t), x(t))$ and a minimizing geodesic $\gamma(\cdot, t)$ connecting these two states (i.e., $\gamma(0,t) = x^*(t)$ and $\gamma(1,t) = x(t)$), solve

$$k^*(x^*(t), \ x(t)) = \underset{u_x \in \mathbb{R}^m}{\text{argmin}} \ \|u_x\|^2$$

$$\text{s.t.} \quad 2\delta_\gamma^T(1,t) M(x(t)) \hat{\dot{x}}(t) - 2\delta_\gamma^T(0,t) M(x^*(t)) \dot{x}^*(t) \leq -2\lambda \mathcal{E}(\gamma(\cdot,t)), \tag{33}$$

where $\hat{\dot{x}}(t) = f(x(t)) + B(x(t))(u^*(t) + u_x)$ represents the nominal dynamics evaluated at $x(t)$ and $\dot{x}^*(t) = f(x^*(t)) + B(x^*(t))u^*(t)$.

A few comments are in order. First, the existence of the dual metric $W(x)$ ensures that there exists a differential feedback controller such that inequality (13) holds for all (x, δ_x) along the minimizing geodesic between x^* and x. Then, by the equivalence shown between expressions (18) and (21), problem $\mathcal{OPT}_{\text{online}}$ is always feasible. Second, the linear inequality (33) is essentially a relaxation of (13), in that it only enforces contraction *tangent to the given geodesic*. In contrast, the differential controller proposed in [9], obtained by solving a *feasibility* problem, must ensure that the system contracts in all directions with *at least* rate λ. Such a relaxation still guarantees IES as only the flow *along the geodesic* affects the convergence of $x(t)$ to $x^*(t)$. On the other hand, such a relaxation can often dramatically decrease control effort as compared with computing the controller using (15). Third, problem $\mathcal{OPT}_{\text{online}}$ is a QP subject to a single linear inequality and thus may be solved analytically (given the geodesic $\gamma(\cdot, t)$). Indeed, the QP above strongly resembles the min-norm formulation of Sontag's generalized formula for CLF-based stabilization [30], thereby underscoring the interpretation of the Riemann energy of the minimizing geodesic as an *incremental* CLF.In Section V we present efficient numerical methods for the geodesic computation.

D. Tracking Control Effort

For systems that satisfy the stronger Killing field condition given by (28), Theorem IV.5 provides a bound on the magnitude of the optimized tracking controller computed using problem $\mathcal{OPT}_{\text{online}}$. We first require the following technical lemma:

Lemma IV.4 (Norm Bound for Tracking Controller)**.** *Let S be a symmetric matrix in $\mathbb{R}^{n \times n}$ and Y a matrix in $\mathbb{R}^{m \times n}$.*

Construct matrices $\overline{Y} \in \mathbb{R}^{n\times m}$ and $\overline{Y}_\perp \in \mathbb{R}^{n\times(n-m)}$ such that the columns of $\overline{Y}$ form an orthonormal basis for the column space of Y^T, i.e., Col(Y^T), and the columns of $\overline{Y}_\perp$ form an orthonormal basis for the nullspace of Y, i.e., $\mathcal{N}(Y)$. Suppose, then, that the following conditions hold:

$$\eta_z^T S\eta_z < 0,\ \forall \eta_z \in \mathcal{N}(Y) \subset \mathbb{R}^n, \tag{34}$$

$$\frac{\theta}{2} \max_{\substack{\overline{\eta}_{z_Y}\in\mathcal{S}^{m-1}\\ \epsilon,\epsilon_\perp\geq 0\\ \epsilon^2+\epsilon_\perp^2\leq 1}} \epsilon\frac{\|\overline{\eta}_{z_Y}\|_{S_Y}^2}{\|Y\overline{Y}\,\overline{\eta}_{z_Y}\|} + 2\epsilon_\perp\frac{\|\overline{Y}_\perp^T S\overline{Y}\,\overline{\eta}_{z_Y}\|}{\|Y\overline{Y}\,\overline{\eta}_{z_Y}\|} < \bar{\delta}_u, \tag{35}$$

for some constants $\bar{\delta}_u \in \mathbb{R}_{>0}$ and $\theta \in \mathbb{R}_{>0}$, where $\mathcal{S}^{m-1}$ denotes the $m-1$ unit sphere, and $S_Y := \overline{Y}^T S\overline{Y}$. Then,

$$\theta\,\eta_z^T S\eta_z < 2\bar{\delta}_u\|Y\eta_z\|, \forall \eta_z\ s.t.\ \|\eta_z\|\leq 1. \tag{36}$$

Proof. Notice first that condition (34) is indeed necessary and sufficient for the inequality in (36) to hold for all $\eta_z \in \mathcal{N}(Y)$. For condition (35), we will first generate an equivalent reformulation of inequality (36) and then demonstrate sufficiency.

Decompose η_z as $\eta_{z_Y} + \eta_{z_{Y_\perp}}$, where $\eta_{z_Y} \in$ Col(Y^T) and $\eta_{z_{Y_\perp}} \in \mathcal{N}(Y)$. Now write $\eta_{z_Y} = \epsilon\hat{\eta}_{z_Y}$ and $\eta_{z_{Y_\perp}} = \epsilon_\perp\hat{\eta}_{z_{Y_\perp}}$ where $\epsilon \in (0,1]$, $0 \leq \epsilon_\perp \leq \sqrt{1-\epsilon^2}$, and $\hat{\eta}_{z_Y}$ and $\hat{\eta}_{z_{Y_\perp}}$ are unit vectors contained in Col(Y^T) and $\mathcal{N}(Y)$, respectively. Substituting these expressions into inequality (36) above yields

$$\theta\left(\epsilon^2\|\hat{\eta}_{z_Y}\|_S^2+\epsilon_\perp^2\|\hat{\eta}_{z_{Y_\perp}}\|_S^2+2\epsilon\epsilon_\perp\hat{\eta}_{z_{Y_\perp}}^T S\hat{\eta}_{z_Y}\right) < 2\bar{\delta}_u\epsilon\|Y\hat{\eta}_{z_Y}\|. \tag{37}$$

Notice now that

$$\max_{\hat{\eta}_{z_{Y_\perp}}\in\mathcal{N}(Y)} \hat{\eta}_{z_{Y_\perp}}^T S\hat{\eta}_{z_Y} = \|\overline{Y}_\perp^T S\hat{\eta}_{z_Y}\|,$$

and by condition (34), $\|\hat{\eta}_{z_{Y_\perp}}\|_S^2 < 0$ for all $\hat{\eta}_{z_{Y_\perp}} \in \mathcal{N}(Y)$. Thus, by upper-bounding the left hand side of the inequality in (37) and rearranging, we obtain the following *sufficient* condition for inequality (36):

$$\frac{\theta}{2}\left(\epsilon\frac{\|\hat{\eta}_{z_Y}\|_S^2}{\|Y\hat{\eta}_{z_Y}\|} + 2\epsilon_\perp\frac{\|\overline{Y}_\perp^T S\hat{\eta}_{z_Y}\|}{\|Y\hat{\eta}_{z_Y}\|}\right) < \bar{\delta}_u, \tag{38}$$

for all $\hat{\eta}_{z_Y} \in$ Col(Y^T). Now, given that the columns of $\overline{Y}$ are an orthonormal basis for Col(Y^T), then $\hat{\eta}_{z_Y}$ may be expressed as $\overline{Y}\overline{\eta}_{z_Y}$ where $\overline{\eta}_{z_Y} \in \mathcal{S}^{m-1}$. Substituting this expression into the inequality above yields (35). □

We now leverage Lemma IV.4 to derive the bound on the magnitude of optimized tracking controller.

Theorem IV.5 (Tracking Control Effort)**.** *Define*

$$F(x) := -\partial_f W(x) + \overline{\frac{\partial f(x)}{\partial x}}W(x) + 2\lambda W(x).$$

Assume the dual CCM $W(x)$ satisfies conditions (28) *and* (29)*. Factorize $W(x)$ as $L(x)^T L(x)$ and define $S(x) = L^{-T}FL^{-1}$ and $Y(x) = B^T L^{-1}$. Suppose then that the matrices $S(x)$ and $Y(x)$ satisfy property* (35) *for all $x \in \mathcal{X}$ with $\theta = \bar{d} = \overline{\alpha}_w\bar{w}/\lambda$, where $\overline{Y}$ and $\overline{Y}_\perp$ are defined as stated in Lemma IV.4. Then, the optimized feedback controller $k^*(x^*, x)$ satisfies the bound:*

$$\|k^*(x^*,x)\| \leq \bar{\delta}_u, \tag{39}$$

for all $x^*, x \in \mathcal{X}$ such that $x \in \Omega(x^*)$.

Proof. As a consequence of CCM condition (29), the matrices $S(x)$ and $Y(x)$ satisfy property (34) for all $x \in \mathcal{X}$. Then, in conjunction with property (35), it follows from the conclusions of Lemma IV.4 that

$$\begin{aligned} \bar{d}^2\eta_z^T\left(L^{-T}FL^{-1}\right)\eta_z < 2\bar{d}\,\bar{\delta}_u\|B^T L^{-1}\eta_z\|,\\ \forall \eta_z\ s.t.\ \|\eta_z\| \leq 1, \end{aligned} \tag{40}$$

for all $x \in \mathcal{X}$. Let $\eta_x := \bar{d}L^{-1}\eta_z$. Then, the set $\{\eta_z \in \mathbb{R}^n : \|\eta_z\| \leq 1\}$ is equivalent to the set $\{\eta_x \in \mathbb{R}^n : \|\eta_x\|_{W(x)}^2 \leq \bar{d}^2\}$ and inequality (40) may be written as

$$\begin{aligned} a(x,\eta_x) < \bar{\delta}_u\|r(x,\eta_x)\|,\\ \forall \eta_x\ s.t.\ \eta_x^T W(x)\eta_x \leq \bar{d}^2, \end{aligned} \tag{41}$$

for all $x \in \mathcal{X}$, where

$$\begin{aligned} a(x,\eta_x) &:= \eta_x^T F(x)\eta_x,\\ r(x,\eta_x) &:= 2B(x)^T\eta_x. \end{aligned}$$

Notice that statement (41) along with the CCM condition (29) is equivalent to the feasibility of the following CLF (with respect to bounded controls) like condition stated in [31]:

$$\inf_{\|\delta_u\|\leq\bar{\delta}_u}\left(a(x,\eta_x) + r(x,\eta_x)^T\delta_u\right) < 0, \tag{42}$$

for all η_x satisfying $\|\eta_x\|_{W(x)}^2 \leq \bar{d}^2$. Then, by Theorem 1 in [31] there exists an almost-smooth function $\delta_u(x,\eta_x)$, bounded in Euclidean norm by $\bar{\delta}_u$, such that condition (42) (equivalently the dual form of inequality (13)) is satisfied for all (x,η_x) along the minimizing geodesic connecting any $x^* \in \bar{\mathcal{X}}$ and $x \in \Omega(x^*)$. For completeness, this function is given below:

$$\delta_u(x,\eta_x) = \begin{cases} 0 & \text{if } r = 0,\\ -\dfrac{a+\sqrt{a^2+\bar{\delta}_u^4\|r\|^4}}{\bar{\delta}_u\|r\|^2\left(1+\sqrt{1+\bar{\delta}_u^2\|r\|^2}\right)}r & \text{else,} \end{cases}$$

where we have dropped the parenthesis (x,η_x) for clarity. For each $x \in \mathcal{X}$, the function above is continuous for all η_x (requisite for integrability) and smooth for $\eta_x \neq 0$.

By the equivalence shown through (20), the tracking controller given by integrating the function above along the minimizing geodesic connecting x^* and x is indeed a feasible solution to problem $\mathcal{OPT}_{\text{online}}$ that satisfies the bound claimed in (39), completing the proof. □

A few comments regarding the computation of the bound $\bar{\delta}_u$ are in order. Note that from Theorem IV.5, one needs to show that inequality (41) holds for all $x \in \mathcal{X}$. Rewriting this inequality as (40), one may deduce a simpler, yet loose approximation of $\bar{\delta}_u$ as:

$$\bar{\delta}_u = \sup_{x\in\mathcal{X}}\left(\frac{\bar{d}\lambda_{\max}(L^{-T}FL^{-1})}{2\underline{\sigma}_{>0}(B^T L^{-1})}\right), \tag{43}$$

where $\underline{\sigma}_{>0}(\cdot)$ denotes the smallest non-zero singular value and $\lambda_{\max}(\cdot)$ the largest eigenvalue. A better approximation may be obtained by leveraging Lemma IV.4 and inequality (35). One would compute $\bar{\delta}_u(x)$ for each $x \in \mathcal{X}$ so that $\bar{\delta}_u = \sup_{x\in\mathcal{X}}\bar{\delta}_u(x)$. For fixed $(\epsilon,\epsilon_\perp)$, the maximization over $\hat{\eta}_{z_Y} \in \mathcal{S}^{m-1}$ in (35) belongs to the class of sum-of-ratios fractional programming and is in general, NP-

complete. Recently in [32], the authors presented a two-stage algorithm using tight SDP relaxations of parameterized sub-problems for maximizing the sum of a generalized Rayleigh quotient and another Rayleigh quotient on the unit sphere. The algorithm is much too intensive for this application however, considering that inequality (35) must be verified for all $x \in \mathcal{X}$. Thus, a suboptimal approximation may be obtained by decoupling the maximization as

$$\max_{\substack{\epsilon,\epsilon_\perp \geq 0 \\ \epsilon^2+\epsilon_\perp^2 \leq 1}} \left(\epsilon \max_{\overline{\eta}_{z_Y} \in \mathcal{S}^{m-1}} \frac{\|\overline{\eta}_{z_Y}\|_{S_Y}^2}{\|Y\overline{Y}\,\overline{\eta}_{z_Y}\|} + 2\epsilon_\perp \max_{\overline{\eta}_{z_Y} \in \mathcal{S}^{m-1}} \frac{\|\overline{Y}_\perp^T S \overline{Y}\,\overline{\eta}_{z_Y}\|}{\|Y\overline{Y}\,\overline{\eta}_{z_Y}\|} \right)$$

The two inner maximizations correspond to maximizing generalized Rayleigh quotients, yielding an outer maximization of an affine expression in $(\epsilon, \epsilon_\perp)$ over a convex set.

V. Numerical Implementation

In this section we discuss numerical methods for the online computation of the geodesic and the solution to problem $\mathcal{OPT}_{\text{online}}$.

Computation of the geodesic between two points $p, q \in \mathcal{X}$ can be framed as the following functional optimization problem:

Optimization Problem $\mathcal{OPT}_\gamma$ — At time $t \geq 0$, given desired state $x^*(t)$ and current state $x(t)$, solve

$$\min_{c(\cdot,t) \in \Gamma(x^*(t), x(t))} \quad \mathcal{E}(c(\cdot,t)) \tag{44}$$

Following the approach in [33], such a problem can be efficiently solved by applying the Chebyshev global pseudospectral method, i.e., by discretizing the interval $[0,1]$ using the Chebyshev-Gauss-Lobatto (CGL) nodes and using Chebyshev interpolating polynomials up to degree N to approximate the solution. The integral in (44) is approximated using the Clenshaw-Curtis quadrature (CCQ) scheme with $K > N$ nodes. As in [33], we choose $K > N$ since the integral involves the inverse of the dual metric W and is not guaranteed to be polynomial.

Given the solution to the geodesic problem $\mathcal{OPT}_\gamma$, parameterized by a set of values $\{\gamma(s_k)\}_{k=0}^K$ and $\{\delta_\gamma(s_k)\}_{k=0}^K$, $s_k \in [0,1]$, problem $\mathcal{OPT}_{\text{online}}$ may now be solved as an analytical QP using $(\gamma(s_k), \delta_\gamma(s_k)), k \in \{0, K\}$.

VI. Numerical Experiments

We now demonstrate our approach on a 6-state planar-quadrotor system (Section VI-A). Also, we show how our results lead to an approach for Tube MPC that boasts several advantages over state-of-the-art counterparts (Section VI-B).

A. Planar Quadrotor

We consider a 6-state planar-quadrotor system, whose dynamics and model parameters can be found in [34, Section 6.6] (omitted due to space limitations). Notably, this system is underactuated and has unstable zero dynamics and thus represents a challenging system to benchmark our approach. By reformulating the dynamics using a body-referenced velocity vector (v_x, v_z), where v_x is the lateral velocity and v_z is the vertical velocity, condition (28) requires that the dual metric $W(x)$ is not a function of v_z or $\dot{\phi}$, the roll-rate. Furthermore, given the translational invariance of the dynamics, $W(x)$ was parameterized as a matrix polynomial up to order 4 in (v_x, ϕ). We impose the state-bounds $(v_x, v_z) \in [-2,2]\times[-1,1]$ m/s and $(\phi, \dot{\phi}) \in [-45^o, 45^o]\times[-60,60]^o/s$, while the propeller thrusts are limited to the range $[0.1, 2]mg$ where m is the mass and g is the gravitational acceleration. We consider as disturbance a cross-wind of magnitude *up to* 0.1 m/s^2. Problem $\mathcal{OPT}_{\widehat{CCM}}$ was solved by sweeping through a range of values for λ, using the parser YALMIP and solver Mosek [35] to solve the SOS programs, each of which took about 60 seconds. Fig. 4 plots the optimal objective of Problem $\mathcal{OPT}_{\widehat{CCM}}$ as a function of λ. The

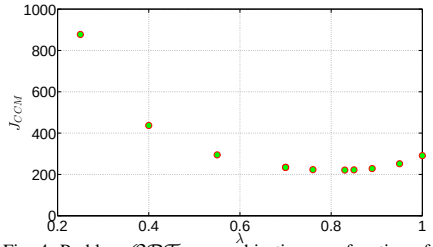

Fig. 4: Problem $\mathcal{OPT}_{\widehat{CCM}}$ objective as a function of λ .

optimal contraction rate was $\lambda = 0.83$. Using gridding, we found that for this example $\overline{\alpha}_w = 0.33$ and $\bar{d} = 0.04$. To put these numbers in perspective, the projection of the outer ellipsoidal approximation of the RCI set onto the $x-z$ plane has a major axis equal to .76 m, and a minor axis equal to .44m, which compare quite favorably with the quadrotor wingspan, equal to .5 m. That is, the size of the RCI tube is rather small and thus the nominal motion planner for the quadrotor is not overly constrained by the tightening of the state constraints.

Having computed (offline) the RCI mapping, we tested Algorithm 1 on the previously unseen densely cluttered environment in Fig. 1. For simplicity, the disturbance here was modeled as a constant perturbing force but the results hold for any bounded time-varying force with varying directionality. Problem MPC is re-solved every $\delta = 1$s with horizon $T = 2$s (using the pseudospectral collocation method and the SNOPT solver) while the tracking controller is implemented using zero-order-hold at 200 Hz. Even using an inefficient implementation in MATLAB, the time required to compute the tracking controller (on a 3.5 GHz Intel equipped with 16 GB of RAM) is on the order of 4ms. In turn, each MPC iteration takes 0.35s. This compares quite favorably with the re-solve time of 1s. Furthermore, we expect that this can be significantly improved with a more efficient implementation and by using trajectory optimization methods that fully exploit the *local* nature of the problem. We do not report the computation of the nominal trajectory (line 6 in Algorithm 1) since it highly depends on the motion planner used and is not a focus of this paper.

This example provides evidence that Algorithm 1 can

be used for the online generation of safe motion plans that can be reliably executed (provided that the nominal motion plan can also be computed in realtime). This example also illustrates the benefits of our method as compared to the funnel library approach [4]. A pre-computed set of trajectories (as required by [4]) would be unlikely to contain a sequence leading from the start to goal while maneuvering through the very tight spaces between obstacles.

B. Application to TMPC

As mentioned in the introduction, the results of this paper can be readily applied in the context of Tube MPC (TMPC). Specifically, consider the canonical problem of stabilization about an equilibrium point (taken to be the origin). To apply our results to TMPC, we modify problem MPC as follows: (1) switch to a running cost of the form $\|x\|_Q^2+\|u\|_R^2$, where $Q \in \mathbb{S}_n$, (2) augment the cost function with a terminal cost $P : \bar{\mathcal{X}}_f \to \mathbb{R}$, and (3) replace the terminal equality constraint (7) with a terminal set constraint, i.e., $\bar{x}(T) \in \mathcal{X}_f \subseteq \bar{\mathcal{X}}$ where $0 \in \mathcal{X}_f$. The terminal set and cost are chosen according to standard stabilization assumptions under the quasi-infinite horizon framework [36], and may be computed using, e.g., LQR. As there is no longer a notion of an initial "motion plan", the reference trajectory is generated in receding horizon fashion by problem MPC and tracked using the CCM-derived feedback controller (also referred to as the "ancillary controller" in TMPC nomenclature).

To compare the resulting approach to TMPC with state-of-the-art methods, we consider the following second-order nonlinear system (taken from [13]):

$$\dot{x}(t) = \begin{bmatrix} -1 & 2 \\ -3 & 4 \end{bmatrix} x + \begin{bmatrix} 0 \\ -0.25x_2^3 \end{bmatrix} + \begin{bmatrix} 0.5 \\ -2 \end{bmatrix} u(t) + \begin{bmatrix} 0 \\ 1 \end{bmatrix} w(t). \tag{45}$$

The control constraints are $|u(t)| \leq 2, \forall t \geq 0$. The state constraints, while not explicitly given in [13], are taken to be the $[-5, 5]^2$ box. The disturbance $w(t)$ is norm bounded ($\|w\| \leq 0.1$), and the state and control cost matrices are $Q = \text{diag}(0.5, 0.5)$ and $R = 1$.

As for the planar-quadrotor example, to obtain a CCM, we solved problem $\mathcal{OPT}_{\widehat{CCM}}$ by sweeping through a range of values for the contraction rate λ. The objective function J_{CCM} was minimized for $\lambda = 1.74$. In particular, we found that the optimized dual metric is in fact constant for all $x \in \mathcal{X}$ (i.e., is a *flat* metric), and is given by:

$$W = \begin{bmatrix} 4.25828 & -0.93423 \\ -0.93423 & 3.76692 \end{bmatrix}.$$

Thus, the RCI mapping is given by the ellipsoid $\Omega(x^*) = \{x \in \mathcal{X} : \|x - x^*)\|_{W^{-1}}^2 \leq 0.093\bar{w}^2\}$. Since here the geodesic between two points is simply given by the straight line connecting those two points (i.e., $\Omega(\cdot)$ is a geodesically convex set), the outer approximation in (27) coincides with the RCI set itself (i.e., $\underline{M} = M = W^{-1}$). Fig. 5 plots the above RCI set using $\bar{w} = 0.1$, along with the RCI set computed in [13] for the same disturbance level (in [13], a *linear* state feedback ancillary controller is used). We observe that our approach yields a markedly smaller invariant set.

We now compare the performance of our method, dubbed

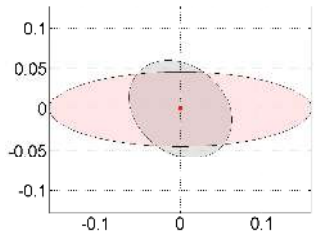

Fig. 5: Comparison of the CCM-derived RCI set (shaded black) and the RCI set computed in [13] (shaded red), centered at the origin, for the same disturbance upper bound $\bar{w} = 0.1$.

contraction-based TMPC, with TMPC methods from [14] and [13] for system (45). In order to ensure fair comparison, we kept the parameters for the the MPC algorithm the same for all three implementations, namely, MPC sample time $\delta = 0.1$s, time horizon $T = 1.5$s, and zero-order-hold sampling time 0.005s. For the tube algorithm in [14], the auxiliary MPC problem was re-solved every $0.05s$ ($\delta/2$). The terminal control invariant set $\mathcal{X}_f$ was also taken from [13] and kept fixed. The initial state was $(3.4, -2.4)$.

Consider the state trajectory plot in Fig. 6, obtained assuming a *constant* disturbance with magnitude 0.1. We present this plot only for our approach. The actual trajectory (in blue) closely tracks the nominal MPC trajectory. Using contraction-based TMPC the state converged to a steady-state value of $(0.0258, 0.006723)$, while the steady-state values using the algorithms from [13] and [14] were found to be $(0.03891, 0.01437)$ and $(0.073, 0.035)$, respectively. While

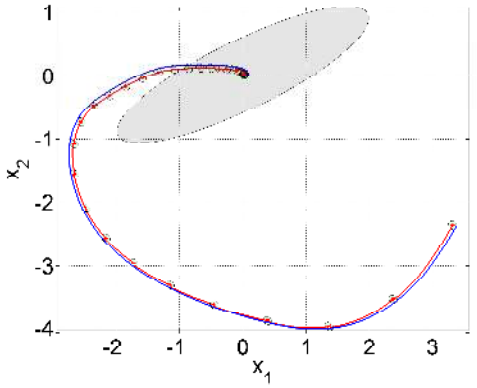

Fig. 6: Closed-loop state trajectory using the optimized ancillary ancillary controller. Red: nominal MPC solution, Blue: actual trajectory. Also plotted is the terminal invariant set (shaded gray) and snapshots of the RCI mapping along the nominal MPC trajectory (green ellipsoids).

the performance characteristics in terms of state-boundedness for all three algorithms are in the same order of magnitude for this example, the "dual-MPC" algorithm from [14] is less suitable for fast, continuous dynamical systems as it essentially requires solving an additional optimal control problem for the ancillary controller (albeit with relaxed constraints) – a heavier computational burden. Relaxing the nominal and/or ancillary re-computation times for this controller led to noticeably worse performance. In contrast, as the CCM is constant and consequently, the minimizing geodesic is simply the straight line between x^* and x, our ancillary feedback controller is entirely analytical. In addition, as mentioned

earlier and in [14], the bound on the deviation of the state from the nominal MPC trajectory is difficult to quantify exactly. Indeed, the cost function for the auxiliary MPC problem required rather ad-hoc tuning to yield acceptable levels of disturbance rejection.

On the other hand, the bound on the ancillary feedback controller derived in [13] is prohibitively high. In particular, the static linear state-feedback law designed in [13] is bounded in absolute value by 0.85. Thus, the restricted control constraints for the nominal MPC must necessarily be $|u^*| \leq 1.15$ (since the total control input is constrained to be $|u| \leq 2$). Under such restrictions, the nominal MPC problem would not even be feasible at the initial state of $(3.4, -2.4)$. In contrast, our optimized ancillary controller satisfies the bound $\|k^*(x^*, x)\| \leq 0.207$, leaving a significantly improved margin of $|u^*| \leq 1.793$ for the nominal MPC input.

In Fig. 7 we compare the feasibility domains for the nominal MPC algorithm using the control constraints: $|u^*| \leq 1.15$ and $|u^*| \leq 1.793$. By analyzing the *intrinsic* properties of the nonlinearities in the system dynamics rather than relying on Lipschitz bounds, we obtained both a significant reduction in the size of the RCI set, and a drastic reduction in the required ancillary control effort, thereby increasing the domain of feasibility for the nominal MPC problem.

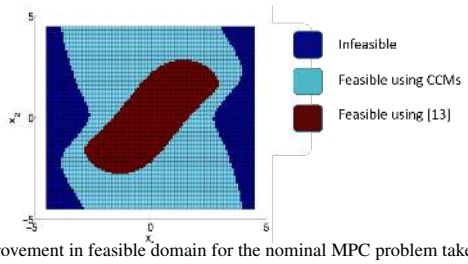

Fig. 7: Improvement in feasible domain for the nominal MPC problem taken from [13].

VII. Conclusions and Future Work

We presented a framework for robust motion planning for robots with nonlinear dynamics subject to bounded disturbances, input constraints, and online state constraints. Our approach allows one to generate certifiably safe trajectories *online* in response to obstacles in the environment. We leveraged recent advances in contraction theory in the form of CCMs to synthesize a tracking feedback controller and an associated fixed-size invariant tube around *any* feasible trajectory. Such an invariant tube can then be used as a robustness margin during online trajectory generation. We demonstrated our approach on a planar quadrotor model navigating through cluttered environments in the presence of cross-wind disturbances. We further discussed applications of our work to TMPC and showed that our approach compares favorably to state-of-the-art nonlinear TMPC algorithms.

Our analysis is generally conservative due to the fact that we derive a *globally valid* invariant tube. A promising approach for reducing this conservatism may be to partition the state space into regions in which CCMs are computed *locally* (while ensuring compatibility between regions). We also plan to extend our work to *stochastic* models of disturbances and sensor noise, which are of practical importance for hardware implementation.

References

[1] R. R. Burridge, A. A. Rizzi, and D. E. Koditschek, "Sequential composition of dynamically dexterous robot behaviors," *Int. Journal of Robotics Research*, vol. 18, no. 6, pp. 534–555, 1999.

[2] R. Tedrake, I. R. Manchester, M. Tobenkin, and J. W. Roberts, "LQR-trees: Feedback motion planning via sums-of-squares verification," *Int. Journal of Robotics Research*, vol. 29, no. 8, pp. 1038–1052, 2010.

[3] A. Majumdar and R. Tedrake, "Robust online motion planning with regions of finite time invariance," in *Workshop on Algorithmic Foundations of Robotics*, 2012.

[4] ——, "Funnel libraries for real-time robust feedback motion planning," 2016, Available at https://arxiv.org/abs/1601.04037.

[5] A. Majumdar, M. M. Tobenkin, and R. Tedrake, "Algebraic verification for parameterized motion planning libraries," in *American Control Conference*, 2012.

[6] M. Althoff and J. Dolan, "Online verification of automated road vehicles using reachability analysis," *IEEE Transactions on Robotics*, vol. 30, no. 4, pp. 903–918, 2014.

[7] J. H. Gillula, H. Huang, M. P. Vitus, and C. J. Tomlin, "Design of guaranteed safe maneuvers using reachable sets: Autonomous quadrotor aerobatics in theory and practice," in *Proc. IEEE Conf. on Robotics and Automation*, 2010.

[8] W. Lohmiller and J.-J. E. Slotine, "On contraction analysis for nonlinear systems," *Automatica*, vol. 34, no. 6, pp. 683–696, 1998.

[9] I. R. Manchester and J.-J. E. Slotine, "Control contraction metrics: Convex and intrinsic criteria for nonlinear feedback design," *IEEE Transactions on Automatic Control*, 2017, In Press.

[10] D. Q. Mayne, "Model predictive control: Recent developments and future promise," *Automatica*, vol. 50, no. 12, pp. 2967–2986, 2014.

[11] M. Kögel and R. Findeisen, "Discrete-time robust model predictive control for continuous-time nonlinear systems," in *American Control Conference*, 2015.

[12] M. Cannon, J. Buerger, B. Kouvaritakis, and S. Rakovic, "Robust tubes in nonlinear model predictive control," *IEEE Transactions on Automatic Control*, vol. 56, no. 8, pp. 1942–1947, 2011.

[13] S. Yu, C. Maier, H. Chen, and F. Allgöwer, "Tube MPC scheme based on robust control invariant set with application to Lipschitz nonlinear systems," *System and Control Letters*, vol. 62, no. 2, pp. 194–200, 2013.

[14] D. Q. Mayne, E. C. Kerrigan, E. J. van Wyk, and P. Falugi, "Tube-based robust nonlinear model predictive control," *Int. Journal of Robust and Nonlinear Control*, vol. 21, no. 11, pp. 1341–1353, 2011.

[15] S. V. Raković, "Set theoretic methods in model predictive control," in *Nonlinear Model Predictive Control*. Springer Berlin Heidelberg, 2009.

[16] F. Bayer, M. Bürger, and F. Allgöwer, "Discrete-time incremental ISS: A framework for robust NMPC," in *European Control Conference*, 2013.

[17] M. Zamani, N. van de Wouw, and R. Majumdar, "Backstepping controller synthesis and characterizations of incremental stability," *System and Control Letters*, vol. 62, no. 10, pp. 949–962, 2013.

[18] S. M. LaValle and J. J. Kuffner, "Randomized kinodynamic planning," *Int. Journal of Robotics Research*, vol. 20, no. 5, pp. 378–400, 2001.

[19] L. Janson, E. Schmerling, A. Clark, and M. Pavone, "Fast Marching Tree: a fast marching sampling-based method for optimal motion planning in many dimensions," *Int. Journal of Robotics Research*, vol. 34, no. 7, pp. 883–921, 2015.

[20] M. E. Villanueva, R. Quirynen, M. Diehl, B. Chachuat, and B. Houska, "Robust MPC via minmax differential inequalities," *Automatica*, vol. 77, no. 1, pp. 311–321, 2017.

[21] J. T. Betts, *Practical Methods for Optimal Control and Estimation using Nonlinear Programming*, 2nd ed. SIAM, 2010.

[22] S. Quinlan and O. Khatib, "Elastic bands: Connecting path planning and control," in *Proc. IEEE Conf. on Robotics and Automation*, 1993.

[23] F. Forni and R. Sepulchre, "A differential Lyapunov framework for contraction analysis," *IEEE Transactions on Automatic Control*, vol. 3, no. 59, pp. 614–628, 2014.

[24] M. Spivak, *A Comprehensive Introduction to Differential Geometry, Vol. I*, 3rd ed. Publish or Perish, Inc., 1999.

[25] J.-i. Itoh and T. Sakai, "Cut loci and distance functions," *Mathematical Journal of Okayama University*, vol. 49, no. 1, pp. 65–92, 2007.
[26] H. K. Khalil, *Nonlinear Systems*, 3rd ed. Prentice Hall, 2002.
[27] I. R. Manchester and J.-J. E. Slotine, "Output-feedback control of nonlinear systems using control contraction metrics and convex optimization," in *Australian Control Conference*, 2014.
[28] P. A. Parrilo, "Semidefinite programming relaxations for semialgebraic problems," *Mathematical Programming*, vol. 96, no. 2, pp. 293–320, 2003.
[29] Z. Lu and T. K. Pong, "Minimizing condition number via convex programming," *SIAM Journal on Matrix Analysis and Applications*, vol. 32, no. 4, pp. 1193–1211, 2011.
[30] J. A. Primbs, V. Nevistić, and J. C. Doyle, "Nonlinear optimal control: A control lyapunov function and receding horizon perspective," *Asian Journal of Control*, vol. 1, no. 1, pp. 14–24, 1999.
[31] Y. Lin and E. D. Sontag, "A universal formula for stabilization with bounded controls," *System and Control Letters*, vol. 16, no. 6, pp. 393–397, 1991.
[32] V.-B. Nguyen, R.-L. Shew, and Y. Xia, "Maximizing the sum of a generalized rayleigh quotient and another rayleigh quotient on the unit sphere via semidefinite programming," *Journal of Global Optimization*, vol. 64, no. 2, pp. 399–416, 2016.
[33] K. Leung and I. R. Manchester, "Chebyshev pseudospectral method for nonlinear stabilization using control contraction metrics," in *American Control Conference*, 2017, to Appear.
[34] J. Steinhardt and R. Tedrake, "Finite-time regional verification of stochastic non-linear systems," *Int. Journal of Robotics Research*, vol. 31, no. 7, pp. 901–923, 2012.
[35] M. ApS, "MOSEK optimization software," Available at https://mosek.com/.
[36] H. Chen and F. Allgöwer, "A quasi-infinite horizon nonlinear model predictive control scheme with guaranteed stability," *Automatica*, vol. 34, no. 10, pp. 1205–1217, 1998.